Crystal Structure and Orientation of Uniaxially and Biaxially Oriented PLA and PP Nanoclay Composite Films

Seyed H. Tabatabaei, Abdellah Ajji

CREPEC, Chemical Engineering Department, Ecole Polytechnique, Centre ville Montreal, Quebec, H3C 3A7 Canada

Received 18 November 2010; accepted 30 August 2011
DOI 10.1002/app.35563
Published online 7 December 2011 in Wiley Online Library (wileyonlinelibrary.com).

ABSTRACT: Cast films of poly(lactic acid) (PLA) and polypropylene (PP) with 2.5 and 5 wt % organo modified nanoclay were prepared and then uniaxially and biaxially hot drawn at $T = 90$ and 155°C, respectively, using a biaxial stretcher. The orientation of PLA and PP crystal unit cells, alignment of clay platelets, as well as the extent of intercalation and exfoliation were studied using wide angle X-ray diffraction (WAXD). The measurement of *d*-spacing of the 001 plane (normal to platelets plane) of the clay tactoids indicated the intercalation of the silicate layers for the PLA nanocomposite films, whereas the PP nanofilled films showed only dispersion of the nanoparticles (i.e., neither intercalation nor exfoliation were observed). The intercalation level of the clay platelets in PLA was almost identical for the uniaxially and biaxially drawn films. Our finding showed that the crystallite unit cell alignments are appreciably dependent on uniaxial and biaxial stretching. Moreover, the incorporation of clay to some extent influenced the orientation of the crystal unit cell axes (*a*, *b*, and *c*) of the oriented films. The silicate layers revealed a much higher orientation into the flow direction in the uniaxially stretched films compared to the biaxially drawn samples. In addition, the orientation of the 001 plane of nanoclays was significantly greater in the PLA compared to the PP nanoclay composite films probably due to a better intercalation and stress transfer in the former. Morphological pictograms illustrating the effects of uniaxial and biaxial stretching on the clay orientation are proposed. © 2011 Wiley Periodicals, Inc. J Appl Polym Sci 124: 4854–4863, 2012

Key words: PLA nanocomposite; PP nanocomposite; orientation; uniaxial drawing; biaxial drawing

INTRODUCTION

It is well established that the effective dispersion of anisotropic particles with high aspect ratios such as short fibers, plates, and whiskers within a continuous polymer matrix, in combination with adequate interfacial adhesion between the filler and polymer, can account for substantially improved reinforcement of the polymer matrix.[1] Layered-silica-based polymer nanocomposites have attracted considerable technological and scientific interest in recent years,[2–5] because they have shown dramatic enhancements in the physical, thermal, mechanical, and barrier properties of polymers even with relatively low loading of silicate.[5–7] These properties are attributed to the layered silicate and confinement of the polymeric matrix at the nano scale.[8] If the silicate tactoids delaminated completely, an exfoliated nanocomposite is obtained. By contrast, if there is only an increase in the interlayer distance, the nanocomposite is termed intercalated.[9] An increased exfoliation of the tactoids results in the formation of a large interface between the soft polymer phase and hard nanoclay platelets. Consequently, the fraction of these rigid particles that is needed to achieve the same effect in properties decreases as exfoliation increases.[10–12] Pioneering advances at Toyota during the early 1990s stimulated the development of various polymer/organosilicate nanocomposites with attractive improved property profiles.[13] Many approaches have been reported to produce organoclay/polyolefin nanocomposites including *in situ* polymerization of monomer in the presence of silicate layers, solvent mixing, and melt compounding.[14] Although *in situ* polymerization proved to be more effective to form exfoliated nanocomposites than melt compounding; however, the exfoliated clay platelets tend to create stacked structures upon subsequent melt processing.[13,14] Therefore, compared with *in situ* polymerization and solvent mixing, melt compounding is the most convenient to prepare polyolefin nanocomposites.[13] The use of organoclays has been extended into different polymer systems including epoxy, polyurethane, polyimides, polyesters, polypropylene, polystyrene, etc.[15]

According to Kaynak and Tasan (2006), various parameters affect the development of nanocomposites; the method for production of nanocomposites,

Correspondence to: A. Ajji (abdellah.ajji@polymtl.ca).
Contract grant sponsors: NSERC (Natural Science and Engineering Research Council of Canada), FQRNT (Fonds Québécois de Recherche en Nature et Technologies).

the type of resin, the type and content of nanoclay, and the chemical modifications used in producing the nanoclay.[16] It has been already elucidated that exfoliated structures could be preferably obtained in polar matrices (e.g., PA and PEO) due to the favorable interactions between the polymer chains and the organo-modified clays.[17,18] Zhong and De Kee (2005) studied structure of blown films of ethylene vinyl acetate (EVA), low density polyethylene (LDPE), and high density polyethylene (HDPE) melt compounded with an organically modified montmorillonite.[14] The morphology analysis showed that all three types of films involve intercalated clay particles while the intercalation extent depended on the type of matrix as well as on the molecular weight of compatibilizers. Wang et al. (2005) investigated the dispersion and orientation of compatibilized injection molded isotactic polypropylene (iPP)/organoclay nanocomposites.[19] A much higher orientation of PP was found in the composites compared to the pristine PP. This was interpreted as due to an enhancement in the local stress that occurred in the inter-particles region of two layered tactoids (platelets) with different velocities. Pereira de Abreu et al. (2007) showed that exfoliation of Cloisite 15A in the polyolefin films can be achieved by optimizing the processing parameters including temperature, processing time, and feed position.[8] The results of their study revealed that the nanoparticles feed position in a twin screw extruder is of vital importance in obtaining an exfoliated film.

Poly(lactic acid) (PLA) is a semicrystalline and biodegradable polymer that can be produced from renewable sources such as corn and whey, which has been considered as a replacement for petrochemical-based materials. Due to its ideal combination of physical properties (high modulus, good film, and fiber forming properties, good heat seal characteristics, and barrier to flavor and aroma) and competitive costs, it is being investigated in a number of commodity applications including flexible packaging (films), fibers, and containers.[20] However, PLA is brittle and exhibits low thermal stability, medium gas barrier, and low solvent resistance against water.[21] As pointed out earlier, the intercalation of nano platelets with high aspect ratio such as layered silicate montmorillonite clay can lead to a pronounced enhancement to the polymer matrix properties in terms of mechanical and barrier.[21] Ray et al. studied the properties of PLA nanoclay composite films.[22,23] They observed an intercalation of the layered silicates that resulted in an improvement in modulus of the nanocomposites and a noticeable reduction in oxygen permeability.

Although few authors have investigated the structure of PLA and PP nanocomposite films in various processes, very little has been conducted on the crystal structure and orientation of uniaxially and biaxially oriented nanocomposite films. In this study, pristine cast films of PLA and PP as well as their nanocomposites with 2.5, 5, and 7.5 wt % nanoclays were produced and then uniaxially and biaxially stretched using a biaxial stretcher machine. A detailed investigation of the effect of uniaxial and biaxial drawing on the crystallite unit cell orientation as well as the nanoclay alignment of the PLA and PP nanocomposite films has been carried out and is presented in this study.

EXPERIMENTAL

Materials

A commercial linear polypropylene (PP) and an extrusion grade commercial poly(lactic acid) (PLA) were selected. PP1274 was supplied by ExxonMobil and had a melt flow rate (MFR) value of 12 g/10 min (under ASTM D1238 conditions of 230°C and 2.16 kg). PLA 2002D was purchased from NatureWorks and had an MFR value of 6 g/10 min. The organically modified montmorillonite clays (Cloisite 30B and Cloisite 20A) supplied by Southern Clay Products were used for PLA and PP, respectively. According to the supplier, in Cloisite 30B, the chemical structure of surfactant is MT2EtOH (methyl, tallow, bis-2-hydroxyethyl, quaternary ammonium chloride) whereas in Cloisite 20A, the chemical structure of surfactant is 2M2HT (dimethyl, dehydrogenated tallow, quaternary ammonium chloride).

Film preparation

Master batches of the PLA and PP containing 10 wt % of nanoclay Cloisite 30B and Cloisite 20A, respectively, were prepared using a twin screw extruder and were diluted to the concentrations of 2.5 and 5 wt %. The cast films were produced by extrusion using a slit die of 1.9 mm thick and 200 mm width where the die temperature was set at 200°C. The stretching was performed on a Bruckner laboratory biaxial stretcher. The initial samples with thickness, width, and length of 1 mm, 10 cm, 10 cm, respectively, were stretched at speed of 10 mm/s simultaneously at the temperatures of 90 and 155°C for the PLA and PP, respectively. The films were uniaxially drawn to a draw ratio of four and biaxially stretched to 4 × 4. After stretching, the films were cooled to room temperature in contact with ambient air.

Film characterization

XRD measurements were carried out using a Bruker AXS X-ray goniometer equipped with a Hi-STAR two-dimensional area detector. The generator was

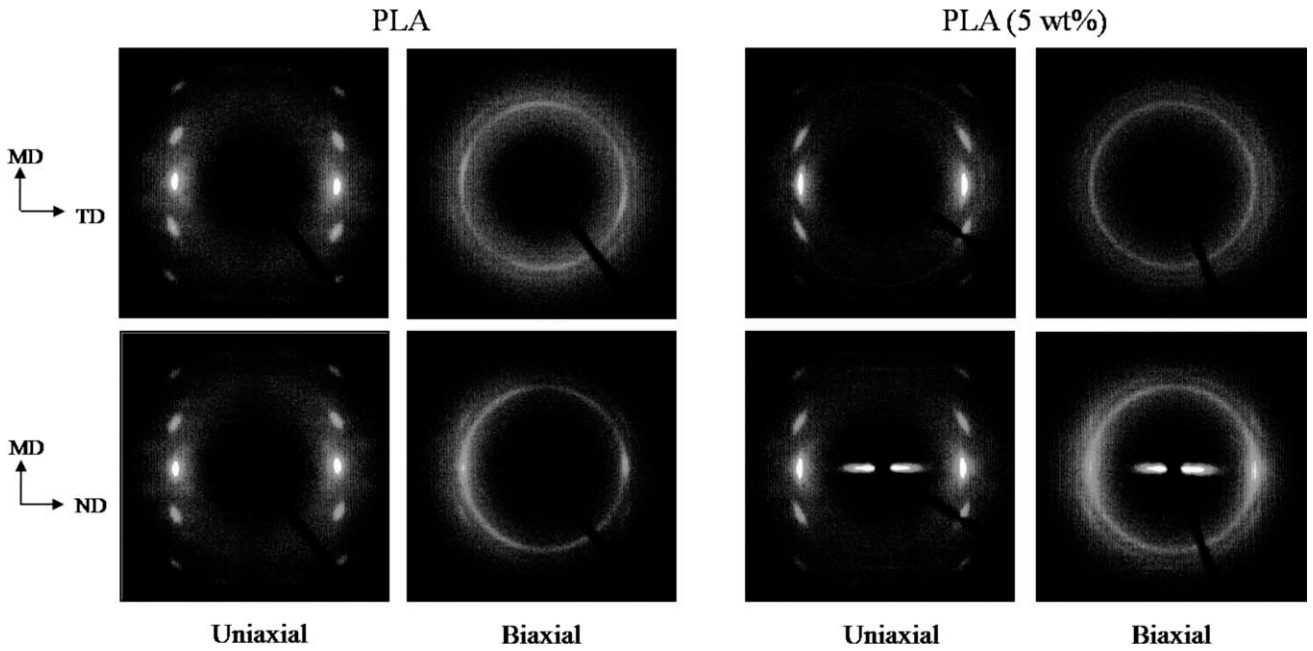

Figure 1 Surface (MD-TD plane) and cross-section (MD-ND plane) 2D WAXD patterns for uniaxially and biaxially oriented neat PLA and PLA (5 wt %-nanoclay) films.

set up at 40 kV and 40 mA and the copper CuKα radiation (λ = 1.542 Å) was selected using a graphite crystal monochromator. The sample to detector distance was fixed at 9.2 cm. To get the maximum diffraction intensity several film layers were stacked together to obtain the total thickness of about 2 mm.

Wide angle X-ray diffraction (WAXD) is based on the diffraction of a monochromatic X-ray beam by the crystallographic planes (*hkl*) of the polymer crystalline phase. Using a pole figure accessory, the intensity of the diffracted radiation for a given *hkl* plane is measured as the sample is rotated through all possible spherical angles with respect to the beam. This allows the determination of the probability distribution of the orientation of the normal to *hkl* plane with respect to the directions of the sample.

The Herman orientation function F_{ij} of a crystalline axis i with respect to a reference axis j is given by:[24]

$$F_{ij} = \frac{(3cos^2(\phi_{ij}) - 1)}{2} \quad (1)$$

where ϕ_{ij} is the angle between the unit cell axes i (a, b, or c) and a reference axis j. The Herman orientation functions were derived from the 110 and 040 pole figures for the PP. Details about the calculations for PP can be found elsewhere.[24] For the PLA, due to overlapping of the 110 and 200 crystalline planes, WAXD cannot be employed for the orientation measurements of the individual unit cell crystal axes. Hence, in this work, the alignments of the 110/200 plane as well as the 203 plane are reported for the PLA.

RESULTS AND DISCUSSION

Since the properties of semicrystalline polymers such as PLA and PP depend on their crystalline structure, in this study, a detailed investigation of the effect of nanoclay and stretching on orientation of the crystallites and nanoparticles were performed using WAXD. Figure 1 shows the surface (MD-TD plane) as well as the cross-section (MD-ND plane). WAXD patterns for the uniaxially and biaxially stretched neat PLA and PLA (5 wt %) nanocomposite films. For PLA, the first and second diffractions at 2θ = 16.6 and 18.9° represent the patterns for the 110/200 and 203 crystalline planes, respectively. As pointed out earlier, due to overlapping of the 110 and 200 crystalline planes of PLA, WAXD cannot be employed for the orientation measurements of crystalline axes (a, b, and c) of PLA. For the uniaxially oriented films, the diffraction pattern demonstrates only arcs that are sharp and concentrated in center, indicating large crystalline orientation. In addition, the diffraction patterns for the surface and cross-section of the uniaxially stretched films are almost similar. However, upon biaxial stretching, a diffraction ring is seen for the 110/200 crystallographic plane of the PLA, indicating low crystalline phase alignment. The diffraction intensity in the equator is somewhat higher in the cross-section than in the surface.

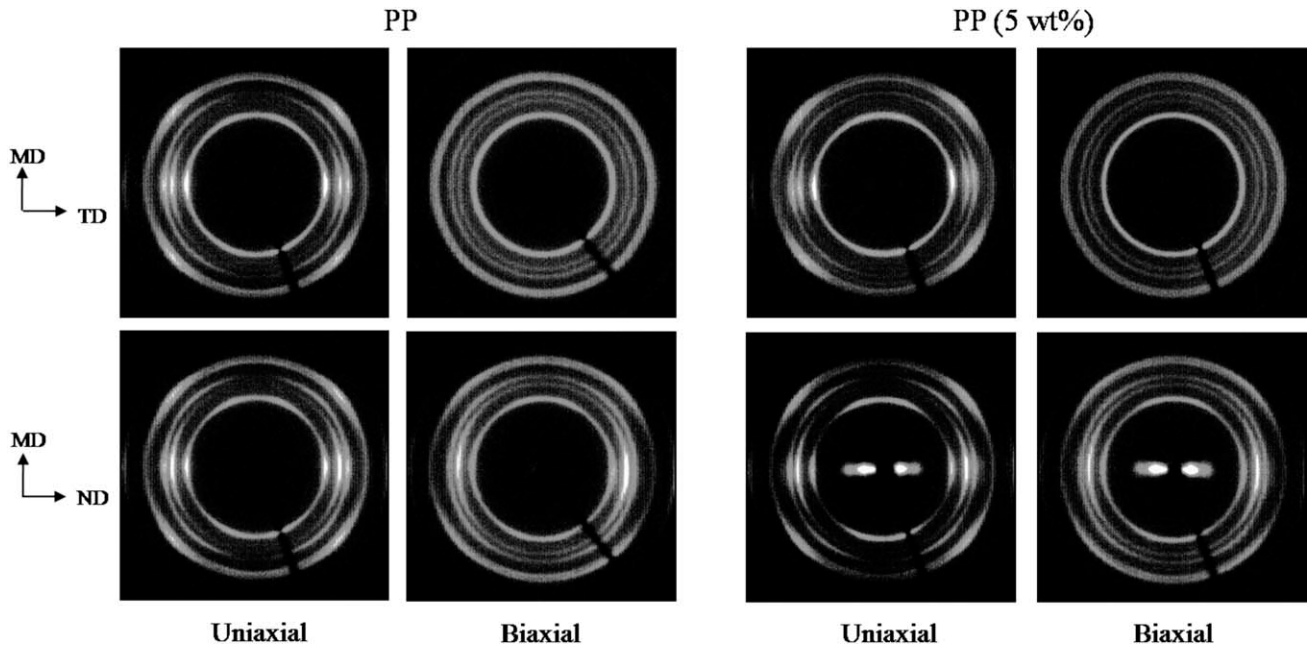

Figure 2 Surface (MD-TD plane) and cross-section (MD-ND plane) 2D WAXD patterns for uniaxially and biaxially oriented neat PP and PP (5 wt %-nanoclay) films.

Additionally, it is obvious that by addition of 5 wt % nanoclay, the arcs are little affected, implying slight changes in crystal orientation in the presence of nanoclay. Figure 1 also elucidates the appearance of equatorial spots in the cross-section patterns of the nanofilled films, indicating that the clay platelets have been well aligned in parallel to the surface of the nanocomposite films.

The surface and cross-section WAXD patterns of the uniaxially and biaxially stretched pristine PP and PP (5 wt %) nanoclay composite films are shown in Figure 2. For the PP, four diffractions at $2\theta = 14.4$, 16.3, 17.4, and 18° are observed corresponding to the 110, 040, 130, and 111 crystallographic planes. Similar trends as were observed for the PLA drawn samples here are observed for the PP oriented films. No orientation of the crystallites is visible in the surface diffraction of the biaxially stretched PP films, whereas some orientation along the equator is detected in their cross-section pattern. This implies that the crystallite unit cells of the biaxially oriented samples have been randomly distributed in the MD-TD plane while slightly aligned into ND. In general, the polymer crystal alignment is governed by the lamellar orientation and/or fibrillar orientation where the unit cell orientation would be higher in the latter.[25] It is well known that the uniaxial drawing of semicrystalline polymers yields a morphological transformation of the spherulites into fibrils at high draw ratios (DR) such as 4.[26] This could explain the high orientation observed for the uniaxially drawn films. However, the crystal lamellae and fibrils are arranged in a network for the biaxially stretched films[27,28] with a considerable fraction of the crystallites having *c*-axis direction lying between MD and TD, leading to a low crystal orientation upon biaxial stretching.

Figure 3 presents the cross-section diffraction intensity profiles of the PLA and PP crystal unit cells as well as the clay for the neat and nanocomposite drawn films. For the PLA [Fig. 3(a)], a major peak at $2\theta = 2.9°$ corresponding to a *d*-spacing of 001 clay plane of 30.5 Å ($d_{001} = \lambda/2 \sin\theta$ where λ is the X-ray wavelength and θ is the diffraction angle) is evident. From the XRD analysis, the original Cloisite 30B clay had a *d*-spacing of 18.5 Å. According to Wang and Wilkie,[29] in an immiscible clay-matrix polymeric mixture, d_{001} must be identical to that of the pure clay, but if an intercalated nanocomposite is formed, d_{001} has to be higher than that of pure clay. Our results show that an intercalation and/or partially exfoliation of the clay particles has been formed in the PLA nanocomposite stretched films. This is attributed to a good affinity between the PLA matrix and Cloisite 30B. As discussed in the material section, the chemical structure of Cloisite 30B has some functional group that enhances its affinity with PLA. On the other hand, several studies[30] reported that PLA and its nanoclay composites do not crystallize easily when quenched from the melt, resulting in the production of films with a low level of crystallinity. It is believed that the nanoparticles can be dispersed much better in amorphous polymers than in crystalline ones from the fact that the crystals prevent the diffusion of the particles during their growth.[30] This could be one of the reasons

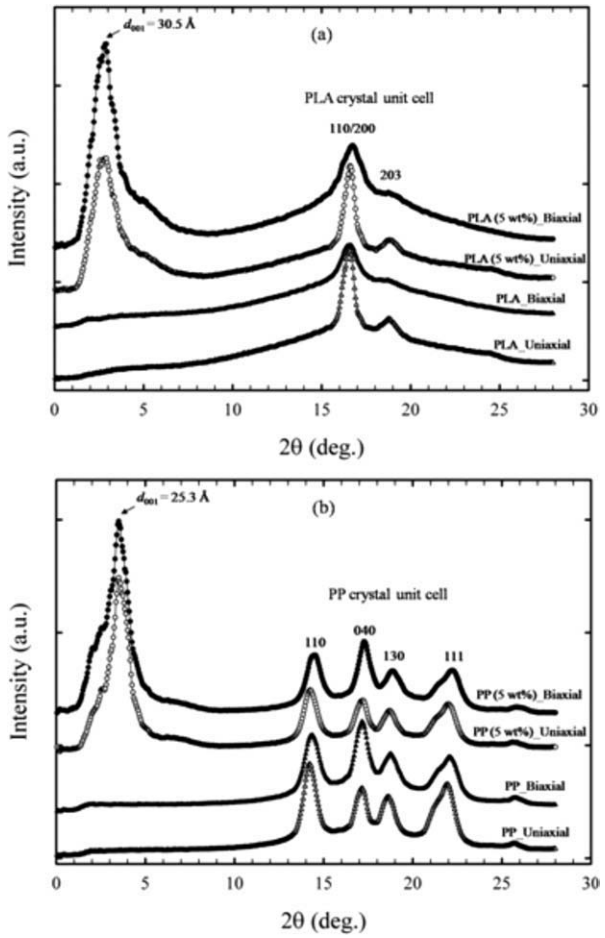

Figure 3 Cross-section diffraction intensity profiles with integration through the circles for uniaxially and biaxially oriented (a) PLA and its nanocomposite films and (b) PP and its nanocomposite films.

explaining why the nanoparticles disperse better in the polymer matrices with a low level of crystallinity (e.g., PLA) than in matrices with a higher crystallinity (e.g., PP). Looking at the diffraction intensity profile of the PLA crystallite [Fig. 3(a)], it should be noted that upon biaxial stretching, the 203 plane intensity decreases and that of the 222 plane at $2\theta = 25.8^\circ$ disappears. For the PP [Fig. 3(b)], a main peak at $2\theta = 3.5^\circ$ corresponding to d_{001} of 25.2 Å is observed. The XRD analysis revealed that the original Cloisite 20A had a *d*-spacing of 24.2 Å. The slight enhancement in the *d*-spacing of the clay tactoids implies that neither intercalation nor exfoliation nanocomposite structure have been formed in the oriented PP films. It is known that PP does not include any polar groups in its backbone and the silicate layers of clay are polar and incompatible with polyolefins.[31] Although different organic cations have been used (e.g., in Cloisite 20A) to change the hydrophilic nature of layered silicates to make them miscible with the hydrophobic character of PP, there still seems to be a gap in compatibility between polypropylene and the organo-modified clay. In Figure 3, the peak positions related to the nanoclays of the uniaxially and biaxially oriented specimens are observed to be almost identical, indicating that the intercalation level of the clay tactoids is somewhat similar for the uniaxially and biaxially drawn films.

The crystalline orientation can be analyzed quantitatively from the WAXD pole figures of the 110/200 and 203 planes for PLA and the 110 and 040 planes for PP and the results are illustrated in Figures 4 and 5, respectively. The normal to the 110 plane is the bisector of the *a* and *b* axes, the normal to 203 is

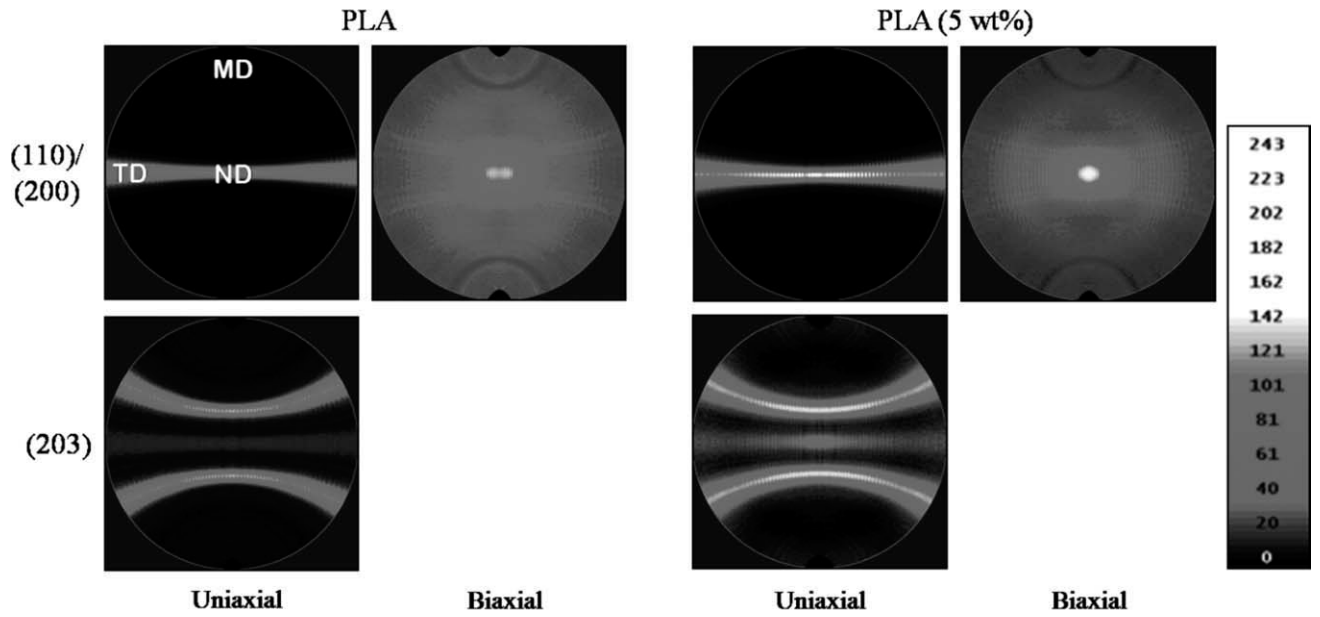

Figure 4 Pole figures of 110/200 and 203 reflections for uniaxially and biaxially oriented neat PLA and PLA (5 wt %-nanoclay) films.

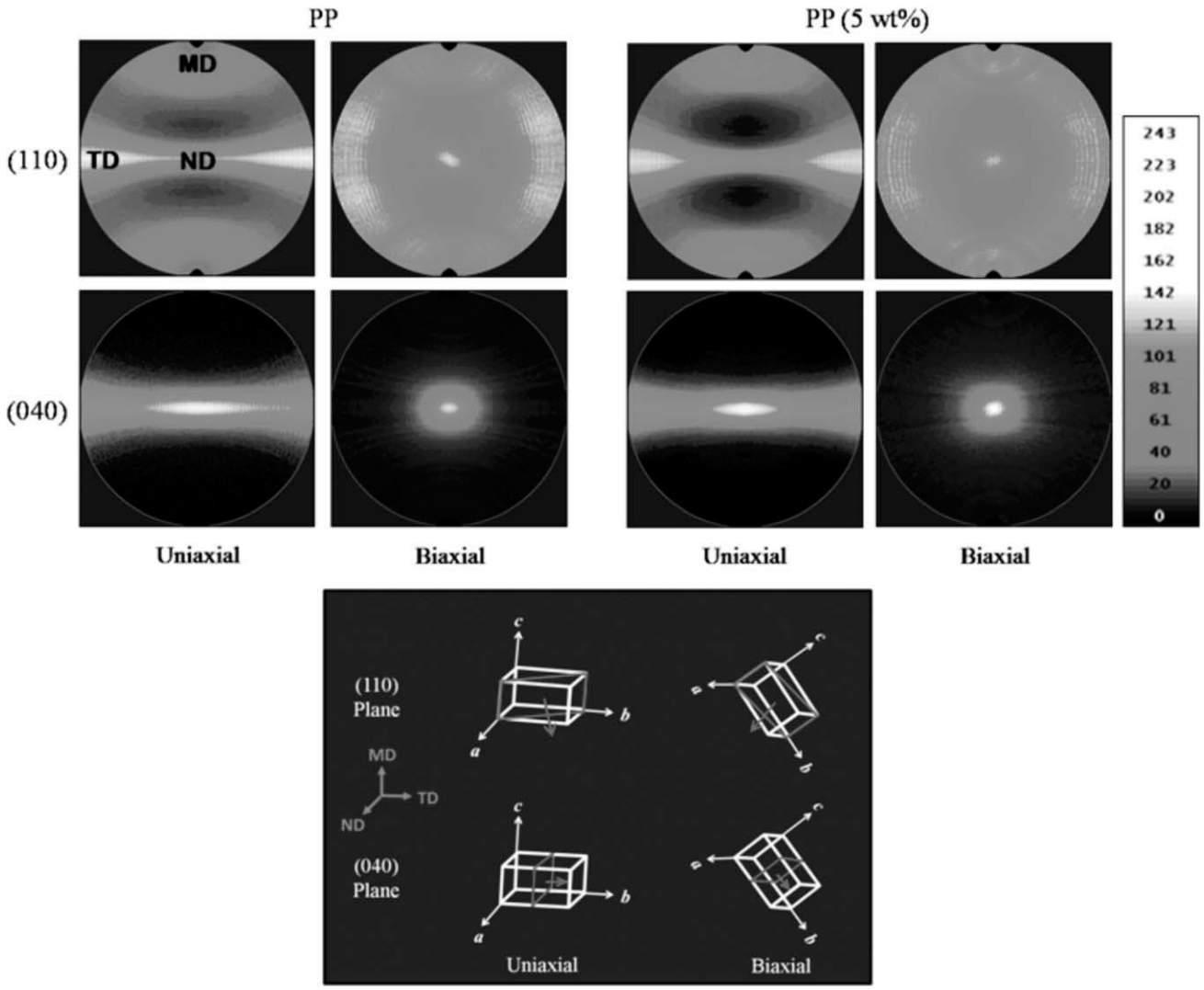

Figure 5 Pole figures of 110 and 040 reflections for uniaxially and biaxially oriented neat PP and PP(5 wt %-nanoclay) films. The schematics in the figure represent the crystal unit cell alignment based on their pole figures for uniaxially and biaxially stretched films.

bisector of the *a* and *c* axes, and 040 is along the *b*-axis of the crystal unit cells.[24] In Figure 4, for both the uniaxially stretched pristine PLA and PLA (5 wt %) nanocomposite samples, significant orientations of the 110/200 and 203 planes in TD and ND are observed. Obviously, for the uniaxially oriented PLA film, the addition of the nanoclay slightly improves the orientation of the 203 plane in ND. However, it is clear that upon biaxial stretching, the 110/200 of the neat PLA and PLA (5 wt %) nanocomposite films appreciably moves to ND. As shown in the PLA diffraction intensity profile of Figure 3(a), for the biaxially stretched PLA films, the 203 diffraction intensity is quite low and as a consequence an accurate determination of its pole figure was impossible.

In Figure 5, for both 0 and 5 wt % clay loadings of the uniaxially drawn PP films, large orientations of the 110 plane in TD and ND and the 040 plane in ND are evident. However, biaxial stretching causes that the 110 plane to be randomly distributed in MD and TD and, to some extent, to be aligned in ND. In addition, the 040 plane is more aligned in ND for the biaxially stretched specimens in comparison with the uniaxially drawn films. The schematics in Figure 5 represent the crystal unit cell alignment based on their pole figures for the uniaxially and biaxially oriented samples. Moreover, it is clear that addition of nanoclay platelets enhances the 040 crystalline plane alignment into ND.

The Herman orientation functions of the 110/200 and 203 planes along MD, TD, and ND for the PLA nanocomposite films are shown in Figure 6. Looking at the orientation data for the 110/200 plane [Fig. 6(a)], it is clear that this plane is almost equally aligned in the TD-ND plane for the uniaxially oriented samples and shows quite low orientation

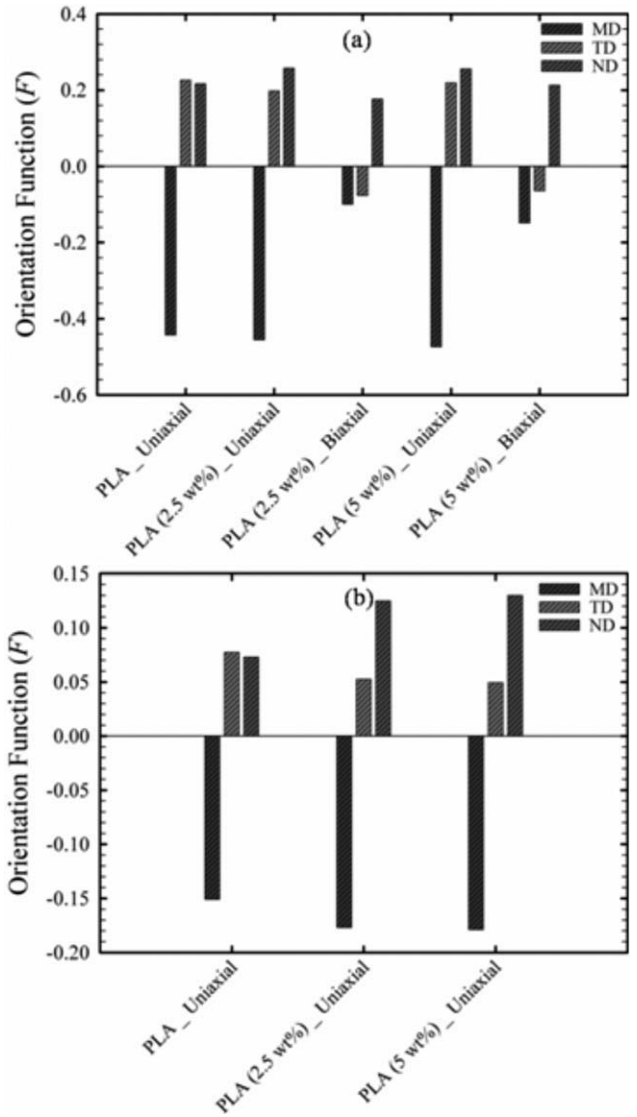

Figure 6 Herman orientation function (F) of the (a) 110/200 and (b) 203 planes with respect to the film axes (i.e., MD, TD, and ND) for uniaxially and biaxially oriented PLA nanocomposite films.

along MD. In addition, obviously, the orientation of the 110/200 plane for the biaxially drawn films is considerably lower than that of the uniaxially stretched samples, whereas its alignment slightly improves by incorporation of nanoclay, confirming the pole figures exhibited in Figure 3. The orientation functions of the 203 plane along ND enhances significantly but reduces slightly in TD upon adding the clay tactoids [see Fig. 6(b)], concluding that the presence of nanoclays promotes to some extent the PLA crystal arrangement. The improvement in polymeric chain orientation in the presence of nanoclays could be due to two reasons[10,32]: (1) shearing experienced by the polymeric chains in the neighborhood of the nanoclay tactoids and (2) significant reduction in the relaxation of oriented chains as a result of the

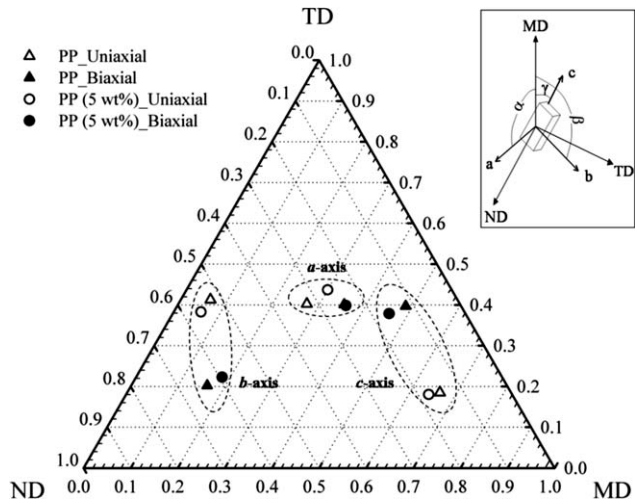

Figure 7 Orientation characteristics as $\cos^2(\phi)$ of the crystal axes (a, b, and c) along MD, TD, and ND for uniaxially and biaxially oriented neat PP and PP (5 wt %).

presence of solid surfaces. In Figure 6(b), it should be noted that 2.5 wt % nanoclay impacts the crystalline orientation whereas further addition of the clay (i.e., 5 wt %) does not drastically alter the orientation characteristics.

The orientation features, in terms of $\cos^2(\phi)$ of the crystalline axes (i.e., a, b, and c, see the sketch in Fig. 7) along MD, TD, and ND obtained from the Herman orientation function for the PP oriented films are plotted in the triangular diagram of Figure 7. It is obvious that for the uniaxially drawn films, the c-axis of the crystals is oriented into MD and the b-axis is close to the TD and ND planes. However, biaxial stretching yields a large movement of the c-axis and b-axis of the crystals toward TD and ND, respectively, and a slight movement of the a-axis into MD. These clearly elucidate a significant

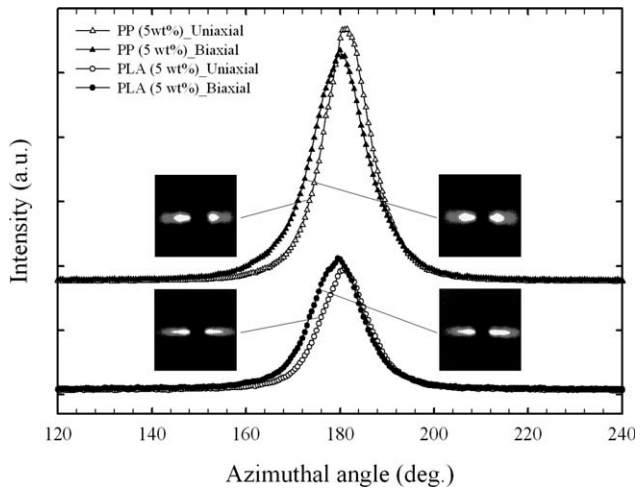

Figure 8 2D WAXD patterns and azimuthal intensity profiles at 2θ of the 001 clay reflection plane for uniaxially and biaxially oriented PLA (5 wt %) and PP (5 wt %).

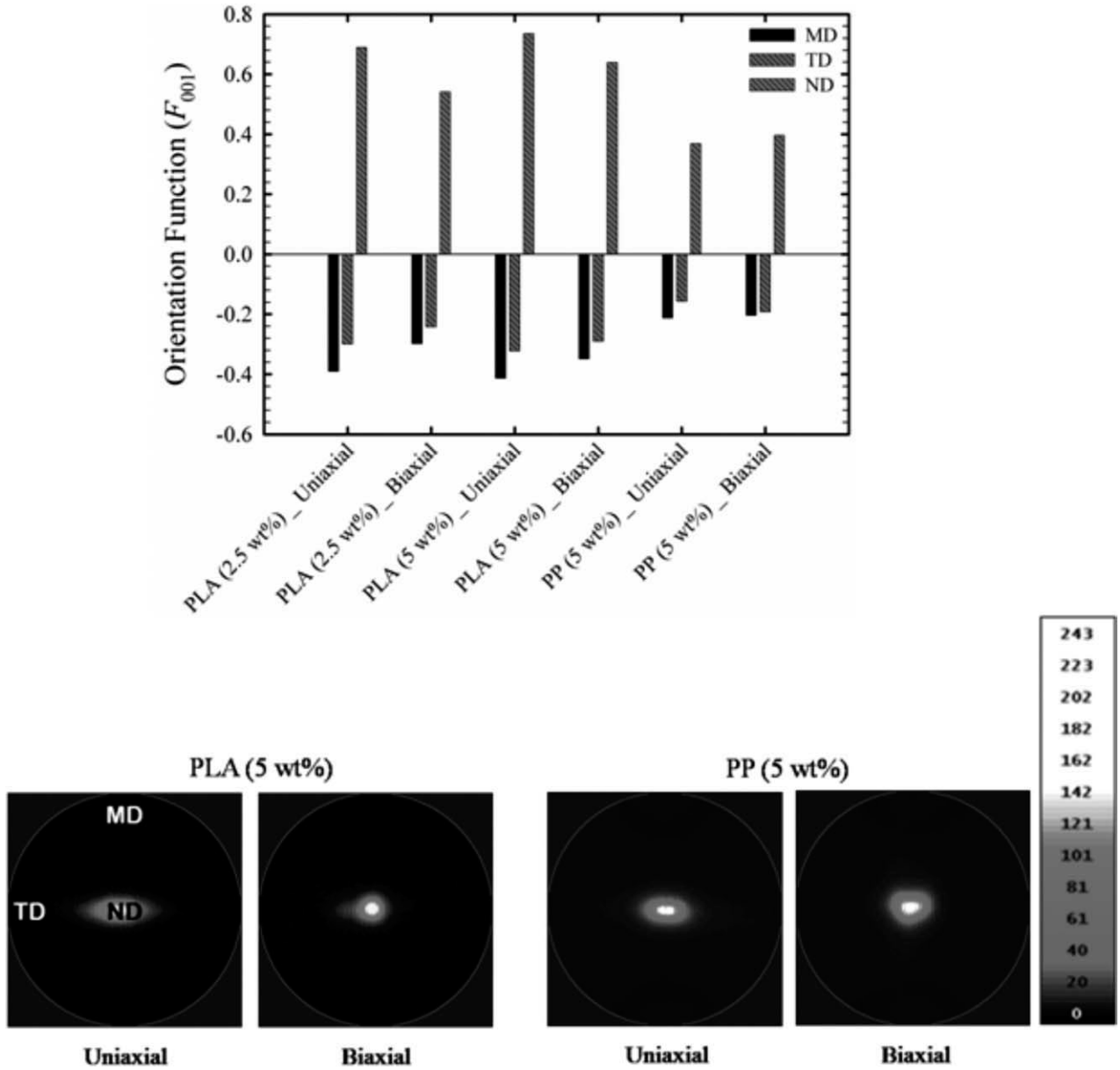

Figure 9 Herman orientation function (F_{001}) (top) and pole figure (bottom) of the 001 plane of clay along MD, TD, and ND for uniaxially and biaxially oriented PLA and PP nanocomposite films.

reduction in orientation along MD upon biaxial drawing, in accordance with the pole figures presented in Figure 5. In addition, it is obvious that the incorporation of the nanofillers has little effect on the orientation of the crystallite axes, confirming our results on the PLA nanocomposite films.

The effect of uniaxial and biaxial drawing on orientation of the clay platelets was also considered using WAXD, as depicted in Figure 8. In the cross-section WAXD patterns, the equatorial bands at $2\theta = 3$–7° are attributed to the clay platelets aligned on the surface of the films. Obviously, the streaks are sharper and more concentrated in the center for the PLA nanocomposite films than the PP films, implying more clay orientation in the former. Moreover, the equatorial streaks are somewhat narrower for the uniaxially drawn films compared with the biaxially stretched samples, indicating a better clay alignment in the former. The qualitative comparison between nanoclay orientation of various samples can be better shown when the intensity is plotted as a function of the azimuthal angle. The azimuthal angle, ϕ, is 0 or 180° along the equator and 90 or 270° along the meridian. For each ϕ, the average intensity at $2\theta = 2$–6° was extracted from the 2D WAXD patterns and the results for the PP and PLA oriented films are plotted in Figure 8. The full width at half maximum (FWHM) is slightly lower for the

uniaxially drawn films, implying higher orientation. Moreover, the greater concentration in the case of PP-clay is indicative of much thicker tactoids, as compared with PLA-clay.

The Herman orientation function (F_{001}) of the 001 plane of the nanoclays for the uniaxially and biaxially oriented PLA and PP nanocomposite films are elucidated in Figure 9. It is obvious that the *c*-axis of the silicate layers is highly aligned in ND, which is also observed from the pole figures of this plane for the PLA and PP oriented samples. Furthermore, it is evident that the *c*-axis of the clay platelets is more aligned into ND for the uniaxially drawn films compared to the biaxially oriented films, supporting the results shown in Figure 8. The orientation of the 001 nanoclay plane increases by increasing nanoclay content, which is consistent with those reported in our previous study[33] on the monolayer PP and multilayer LLDPE/PP-nanoclay/LLDPE nanocomposite blown films. In addition, in Figure 9, clearly, the nanofiller alignment for the PLA films is much greater than those for the PP. This is probably due to a better intercalation of the clay particles in the PLA than in the PP and as a consequence a better stress transfer in the former. According to Zhong and De Kee, clay orientation in shear flow is highly dependent on the matrix flow behavior and to a lower extent on the clay structural state, in accordance with the present study.[14] As shown in the experimental section, the MFR of PLA is lower than that of PP, which means that at the same compounding temperature, the PLA viscosity is higher than that of PP. This is a favorable factor for both better clay dispersion and better clay particle alignment in PLA.

Based on our observations from XRD analyses, two pictograms (one for uniaxially stretched films and the other for biaxially oriented ones) illustrating the orientation of the clay platelets with respect to the film axes (i.e., MD, TD, and ND) are proposed, as depicted in Figure 10. The results of the *d*-spacing of the nanoparticles showed an intercalated clay structure for the PLA nanocomposite films. For the uniaxially drawn films, WAXD patterns, pole figures as well as clay orientation data (Figs. 8 and 9) suggest that the clay platelets have been well aligned in MD-TD plane [see Fig. 10(a)] where normals to the clay platelet are along ND. However, in the biaxially oriented films, the alignment of normals to the clay platelets drastically reduces along ND and noticeably improves in MD and TD [see Fig. 10(b)]. All these, as discussed, could be related to the different crystalline structure formed upon uniaxial and biaxial drawing. As described above, in uniaxial stretching, the spherulitic crystal structure of the unstretched films is transformed into the fibrillar form. This transformation leads to a high alignment of the nanoclays into the deformation direction. However, upon biaxial drawing, the crystal lamellae and fibrils are arranged in a network, resulting in a less alignment of the clay in the MD-TD plane.

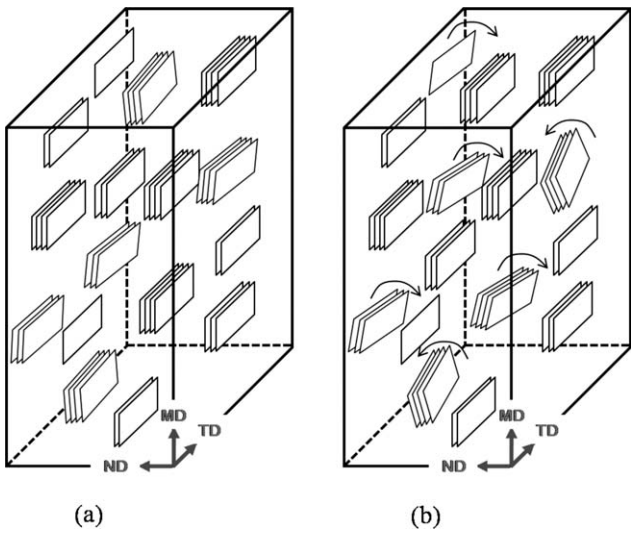

Figure 10 Schematic of the orientation of clay tactoids for (a) uniaxially and (b) biaxially oriented nanocomposite films.

CONCLUSIONS

In this work, we have investigated the orientation of crystallite unit cell axes, the alignment of clay platelets as well as the extent of intercalation and exfoliation in uniaxially and biaxially oriented PLA and PP nanoclay composite films. The measurement of *d*-spacing of the 001 plane of the clay tactoids indicated the intercalation of the silicate layers for the PLA nanocomposite films whereas the PP nanofilled films showed only dispersion of the nanoparticles. The results showed that the crystallite unit cell alignments are appreciably dependent on uniaxial or biaxial stretching. The incorporation of clay slightly enhanced the orientation of the crystallite unit cell of the oriented films possibly due to shearing experienced by the polymeric chains in the neighborhood of the nanoclay tactoids and significant reduction in the relaxation of oriented chains as a result of the presence of solid surfaces. The silicate layers revealed a much higher orientation in the flow direction in the uniaxially stretched films compared to the biaxially drawn ones. This was explained as due to the fibrillar crystalline structure formed in the uniaxially oriented films and random arrangement of the crystal lamellae and fibrils for the biaxially drawn films. The orientation of the 001 plane of nanoclays was significantly greater in the PLA compared to the PP nanoclay composite films, probably due to a better intercalation of nanofillers in the former and as a consequence a better stress transfer.

References

1. Katz, H. S.; Milewski, J. V. In Handbook of Filler for Plastics; Reinhold, V. N. Eds. Van Nostrand Reinhold: New York, 1999.
2. Giannelis, E. P. Adv Mater 1996, 8, 29.
3. Giannelis, E. P.; Krishnamoorti, R.; Manias, E. Adv Polym Sci 1995, 33, 107.
4. Krishnamoorti, E.; Vaia, R. A.; Giannelis, E. P. Chem Mater 1996, 8, 1728.
5. Kojima, Y.; Usuki, A.; Kawasumi, M.; Okada, A.; Fukushima, Y.; Kurauchi, T.; Kamigaito, O. J Mater Res 1993, 8, 1185.
6. Jiang, L.; Wei, K. J Appl Phys 2002, 92, 6219.
7. Wang, S.; Hu, Y.; Qu, Z.; Wang, Z.; Chen, Z.; Fan, W. Mater Lett 2003, 57, 2675.
8. Pereira de Abreu, D. A.; Paseiro Losada, P.; Angulo, I.; Cruz, J. M. Eur Polym J 2007, 43, 2229.
9. Scaffaro, R.; Botta, L.; Paolo La Mantia, F. Macromol Mater Eng 2009, 294, 445.
10. Fujiyama-Novak, J. H.; Cakmak, M. Macromolecules 2008, 41, 6444.
11. Lee, K. M.; Han, C. D. Polymer 2004, 44, 4573.
12. Ergungor, Z.; Cakmak, M.; Batur, C. Macromol Symp 2002, 185, 259.
13. Okada, A.; Kojima, Y.; Kawasumi, M.; Fukushima, Y.; Kuranchi, T.; Kamigaito, O. J Mater Res 1993, 8, 1179.
14. Zhong, Y.; De Kee, D. Polym Eng Sci 2005, 45, 469.
15. Lebaron, P. C.; Wang, Z.; Pinnavaia, T. J Appl Clay Sci 1999, 15, 11.
16. Kaynak, C.; Tasan, C. Eur Polym J 2006, 42, 1908.
17. Picard, E.; Vermogen, A.; Gerard, J. F.; Espuche, E. J Membr Sci 2007, 292, 133.
18. Miltner, H. E.; Assche, G. V.; Pozsgay, A.; Pukansky, B.; Van Mele, B. Polymer 2006, 47, 826.
19. Wang, K.; Xiao, Y.; Na, B.; Tan, H.; Zhang, Q.; Fu, Q. Polymer 2005, 46, 9022.
20. Smith, P. B.; Leugers, A.; Kang, S.; Yang, X.; Hsu, S. L. Macromol Symp 2001, 175, 81.
21. Rhim, J. W.; Hong, S. I.; Ha, C. S. Food Sci Technol 2009, 42, 612.
22. Ray, S. S.; Maiti, P.; Okamoto, M.; Yamada, K.; Ueda, K. Macromolecules 2002, 35, 3104.
23. Ray, S. S.; Yamada, K.; Okamoto, M.; Ogami, A.; Ueda, K. Polymer 2003, 44, 6633.
24. Alexander, L. E. X-ray Diffraction Methods in Polymer Science; Wiley Interscience: New York, 1969.
25. Bafna, G.; Beaucage, G.; Mirabella, F.; Mehta, S. Polymer 2003, 44, 1103.
26. Tabatabaei, S. H.; Carreau, P. J.; Ajji, A. Polymer 2009, 50, 3981.
27. Lupke, T.; Dunger, S.; Sanze, J.; Radusch, H. J. Polymer 2004, 45, 6861.
28. Brandrup, J.; Immergut, E. H.; Grulke, E. A. Polymer Handbook; Wiley: New York, 1999.
29. Wang, D.; Wilkie, C. Polym Degrad Stabil 2003, 80, 171.
30. Wu, D.; Wu, L.; Yu, W.; Xu, B.; Zhang, M. Polym Int 2009, 58, 430.
31. Liu, X.; Wu, Q. Polymer 2001, 42, 10013.
32. Hwang, W. R.; Peters, G. W. M.; Hulsen, M. A.; Meijer, H. E. H. Macromolecules 2006, 39, 8389.
33. Tabatabaei S. H.; Ajji A. J Plast Film Sheet 2011, 27, 87.